World Scientific
www.worldscientific.com

Effect of grain size on thermal shock property of alumina ceramic

Xianghong Xu*, Shilong Sheng, Wenjun Yuan and Zhongkang Lin

State Key Laboratory of Nonlinear Mechanics (LNM)
Institute of Mechanics, Chinese Academy of Sciences
Beijing 100190, P. R. China
*xxh@lnm.imech.ac.cn

Ceramic has a great broad application in high-temperature environment due to its favorable mechanical, antioxidant and corrosion resistance properties. However, it tends to exhibit severe crack or fail under thermal shock resulting from its inherent brittleness. Microstructure property is a vital factor and plays a critical role in influencing thermal shock property of ceramic. The present study experimentally tested and characterized thermal-shock crack and residual strength of ceramic under different quench temperature, while two kinds of alumina ceramics with different grain size are employed. A two-dimensional (2D) numerical model based on statistical mesoscopic damage mechanics is introduced to depict the micro-crack propagation of ceramic sheet under water quenching. The effects of grain size on critical thermal shock temperature, crack characteristics and residual strength are studied. And the microscopic mechanism of the influence of grain size on thermal shock resistance of ceramic is discussed based on the crack propagation path obtained from experimental and simulation results. The qualitative effect and evolution change of grain size on thermal shock property of alumina ceramic will be summarized.

Keywords: Ceramic; grain size; thermal shock.

1. Introduction

Ceramics have been widely applied in high-temperature environment as one of the most popularly structural materials due to their favorable properties such as high mechanical, antioxidant and corrosion resistance properties. However, ceramics exhibit low resistance to fracture by thermal shock due to their brittleness, and often occur in cracking or worse, even a highly catastrophic failure. It could bring great inconvenience to the production and life of people. How to improve thermal shock resistance of ceramics is one of the urgent engineering problems. Microstructure design is regarded as one of the dominant themes in improving the thermal shock resistance of ceramics.

*Corresponding author.

As known, grain size would influence the thermal shock properties of ceramic materials. This has been found by Gupta [1972], Seaton and Dutta [1974] and Carolan *et al.* [2012] experimenting with Al_2O_3 [Gupta, 1972], B_4C [Seaton and Dutta, 1974] and PCBN [Carolan *et al.*, 2012], respectively. The reduction of residual strength transits from discontinuous to continuous as the grain size increases. Gupta [1972] made a qualitatively description of the extent of crack propagation decreasing with increasing grain size of Al_2O_3. Seaton and Dutta [1974] found that increasing the grain size of thermally shocked B_4C from $2\,\mu m$ to $16\,\mu m$ could decrease the critical thermal shock temperature from $225°C$ to $150°C$. Carolan *et al.* [2012] theoretically calculated the critical temperatures which agree well with the observed experimental data for PCBN material when a flaw size equal to the CBN grain size is employed. Hasselman's unified theory [Hasselman, 1969] pointed out that dynamic extended cracks show a tendency towards quasi-static propagation as increasing Griffith flaw size which corresponds to the grain size. Bayuseno *et al.* [1999] experimentally found that the coarse-grained material has higher thermal shock resistance parameter than the fine-grained one for its lesser decrease of the residual strength. You *et al.* [2005] indicated that fine grain can improve the mechanical properties and thermal shock resistance of Al_2O_3/TiC composites, such as the critical thermal shock temperature can be improved about $100°C$ higher than that of the monolithic alumina by controlling the starting powder size. Wang *et al.* [2001] found that the coarse-grained alumina has a greater resistance to thermal shock than fine-grained alumina in terms of the higher critical quench temperature which is due to its higher thermal shock fracture factors.

In fact, the thermal shock process is the interior flaws of materials propagate under thermal stress until cracking. Thermal shock cracking is the main reason for the residual strength of thermal-shocked ceramic decreases. Most of the previous researches focus on studying the effect of the grain size on the extending process of cracks under thermal shock. In the present study, the effects of grain size on the thermal shock properties, such as critical thermal shock temperature, crack characteristics and residual strength, are studied. And the microscopic mechanism of the influence of grain size on thermal shock resistance of ceramic is discussed based on the crack propagation path.

2. Experiment Details

Two kinds of alumina ceramics with different grain size were prepared. The fine-grained and coarse-grained alumina materials were sintered under $30\,MPa$ pressure at $1550°C$ and $1600°C$, respectively, by a spark plasma sintering technique with corresponding starting alumina powder size of $0.14\,\mu m$ and $30\,\mu m$. The grain sizes of sintered alumina ceramics are about $4.1 \pm 1.7\,\mu m$ and $25.3 \pm 13.3\,\mu m$, respectively (as presented in Fig. 1). The alumina bulks were cut into bars with dimensions of $50 \times 6 \times 1\,mm^3$ (as revealed in Fig. 2). The ceramic sheets were ground and polished,
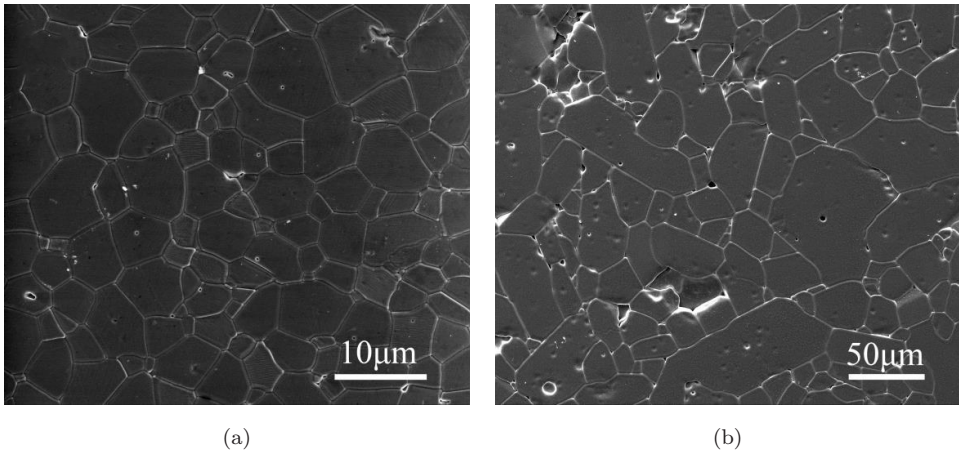
Fig. 1.   SEM microstructures of alumina with different grain size. (a) $4.1 \pm 1.7 \, \mu$m and (b) $25.3 \pm 13.3 \, \mu$m.
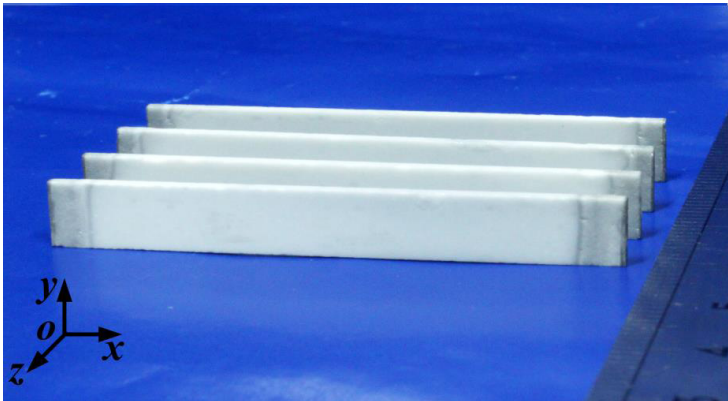

Fig. 2.   Ceramic sheets for thermal shock with specimen sizes $50 \times 6 \times 1 \, \text{mm}^3$.

slightly chamfered, then stacked to prevent coolant accessing the interior surfaces, as shown in Fig. 3.

The stacks were firstly heated in a muffle furnace (MF-0914P) at a rate of $15°$C/min to a pre-determined temperature and kept for 20 min, then quenched in water at $17°$C by free fall. The arrow indicated the free fall direction for thermal shock, as presented in Fig. 3. The quenched samples were dried and then dyed with blue ink to characterize and record the formed cracks. The crack patterns on the interior surface of each sample after quenching were photographed by a digital scanner (Figs. 4 and 5). The maximum vertical distance from the tip of a crack to the side was defined as crack depth and its dimensionless expression was obtained by dividing by half the sample height (3 mm). Using the group average method
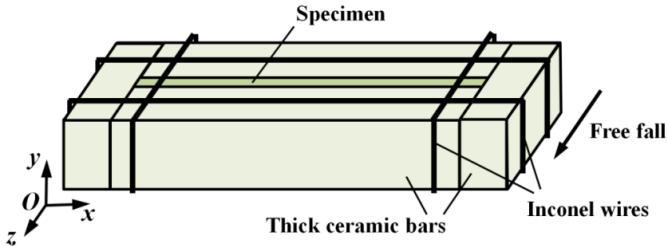
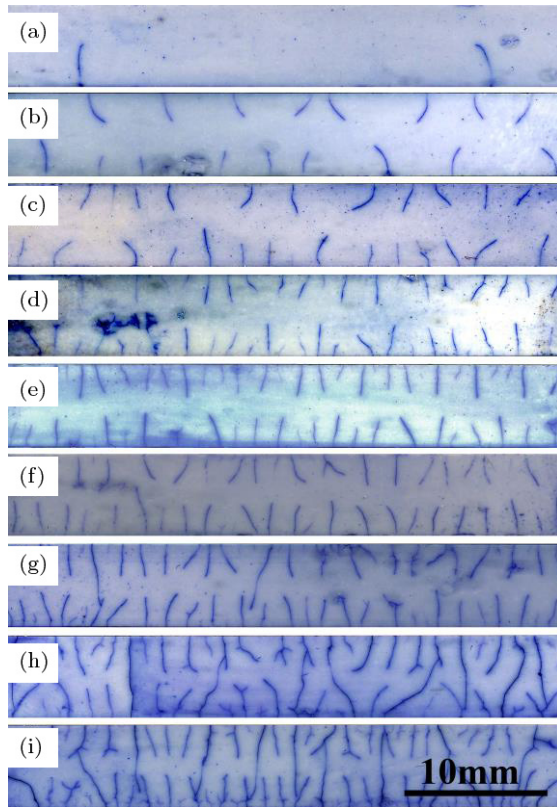Fig. 3.   Schematic of bound specimen and free fall direction for thermal shock.

Fig. 4.   Crack patterns on the interior surface of quenched ceramic sheets with grain size 4.1 μm. The quenching temperature is (a) 240°C; (b) 270°C; (c) 300°C; (d) 350°C; (e) 400°C; (f) 500°C; (g) 500°C (with penetrating cracks); (h) 600°C and (i) 700°C.

[Sokal and Michener, 1958], the cracks with length grading structure can be divided into long cracks and short cracks. Cracks with depths greater than 0.39 and 0.40, respectively for fine-grained ceramic and coarse-grained ceramic, were defined as the long cracks which play a major role on the residual strength of shocked specimens. The mean values of the depth and density of the long cracks versus the quench
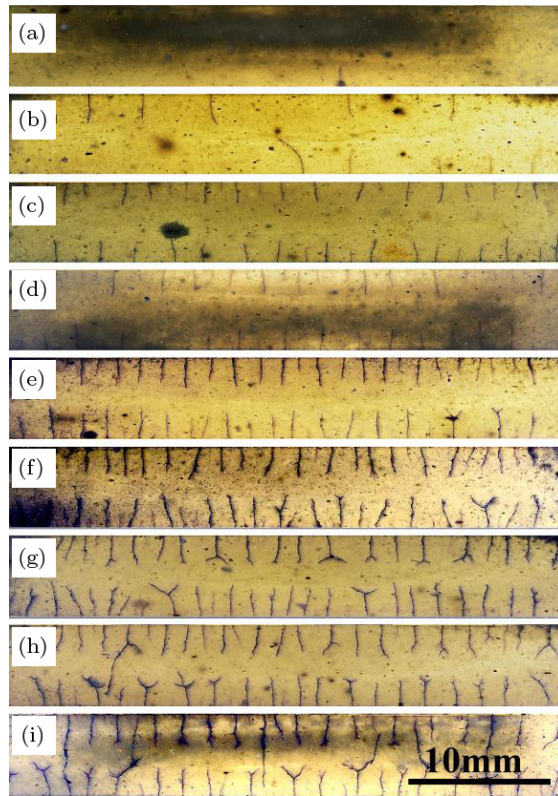
Fig. 5.   Crack patterns on the interior surface of quenched ceramic sheets with grain size 25.3 μm; The quenching temperature is (a) 220°C; (b) 240°C; (c) 270°C; (d) 300°C; (e) 400°C; (f) 500°C; (g) 600°C; (h) 600°C (with penetrating cracks) and (i) 700°C.

temperature are shown in Figs. 6 and 7, respectively. To remove boundary effects, 5 mm sections near each end of the ceramic sheets were excluded from the statistical range. Five samples were selected to measure and analyze the crack characteristics to avoid the occasional cases at each point.

After the shocked specimens were dried at 110°C for 2 h, the residual strength was measured by the three-point bending test (Instron 5848) with a crosshead speed of 0.5 mm/min and a loading span of 30 mm. The experimental results of the residual strength versus quench temperature are plotted in Fig. 8.

Moreover, the microstructure of the thermal-shock crack propagation path was investigated. The surface of the ceramic sheet was first ground and polished into a mirror surface and thermal etched in the muffle furnace at 1550°C for 30 min. After that, the surface etched sheets were quenched at a predetermined temperature and the thermal shock cracks were observed by an optical microscope (KEYENCE VHX-5000). Figure 9 shows the photograph of the cracks at the quench temperature of 300°C, 500°C and 700°C.
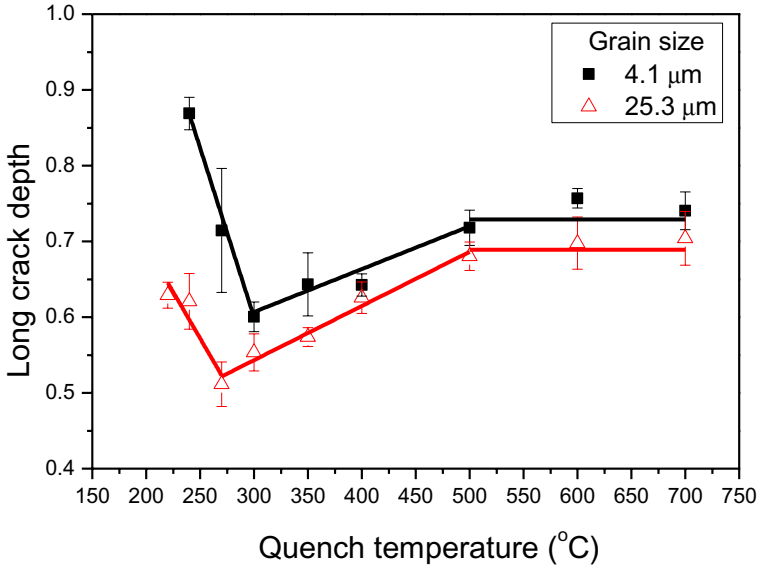
Fig. 6. Normalized long crack depth of quenched ceramic sheets as a function of quench temperature.
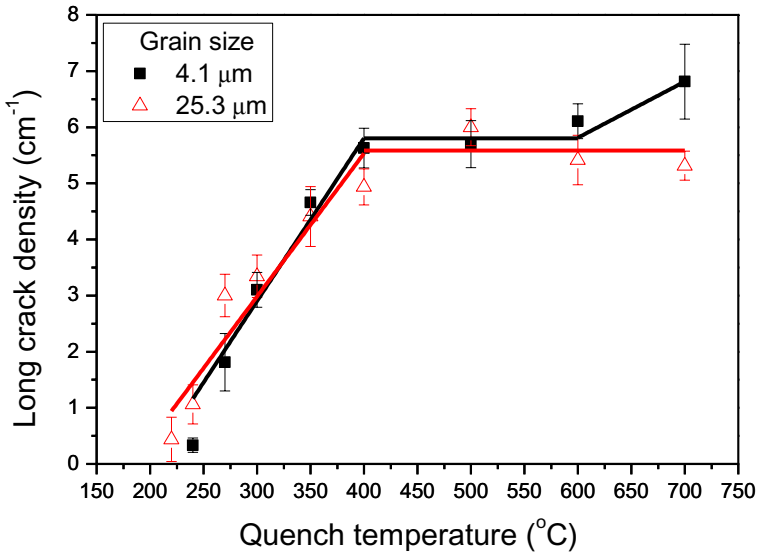

Fig. 7. Long crack density of quenched ceramic sheets versus quench temperature.

Experimental results reveal that the critical thermal shock temperature (T_c) suggested that the first thermal shock cracks occurred at 240°C and 220°C, respectively, for the fine-grained and coarse-grained Al_2O_3 (as presented in Figs. 4 and 5). As the quench temperature $T < T_c$, the values of residual strength are equal to
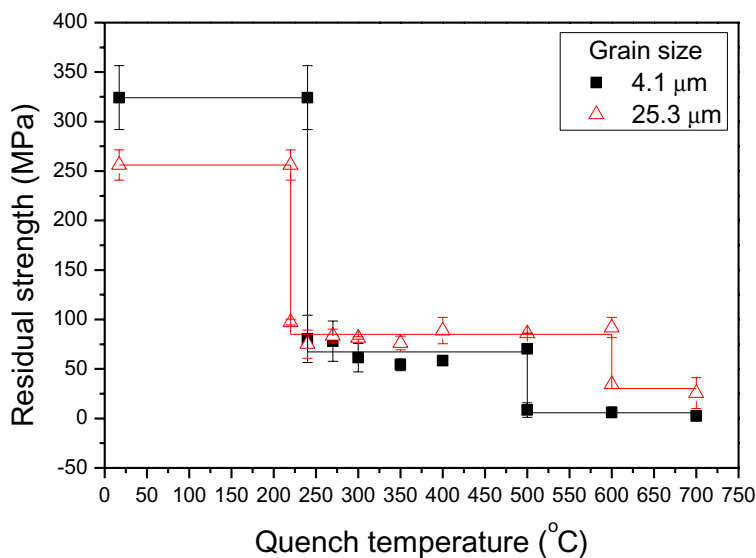
Fig. 8.   Residual strength of quenched ceramic sheets versus quench temperature.

the initial strength since no cracking was detected. The initial strengths of the fine-grained and coarse-grained Al_2O_3 were 324.2 MPa and 256.2 MPa, respectively (as presented in Fig. 8). The fine-grained Al_2O_3 has a higher critical thermal shock temperature than the coarse-grained Al_2O_3, which is mainly attributes to its higher initial strength. This result is similar to what was reported with that for B_4C given by Seaton and Dutta [1974].

As the quench temperature $T = T_c$, the residual strength experienced the first reduction by the initiation of thermal shock cracks. The residual strengths of the fine-grained and coarse-grained Al_2O_3 are 67.2 MPa and 85.0 MPa with the reduction ratio of 79.3% and 66.8%, respectively (Fig. 8). As T increased to the second critical thermal shock temperature, 500°C and 600°C respectively for the two kinds of alumina, the residual strength experienced the second reduction by the initiation of penetrating cracks (Figs. 4(g), 5(h) and 8). The penetrating cracks often get through the centerline of the specimen, connect with the cracks initiating from the opposite edge, and lead to a loss of load-bearing capacity. The residual strengths of the fine-grained and coarse-grained Al_2O_3 were 5.7 MPa and 30.1 MPa with the reduction ratio of 98.2% and 88.3%, respectively (Fig. 8). The residual strength of the coarse-grained alumina is always larger than that of the fine-grained alumina at each quench temperature as $T \geq T_c$. The coarse-grained Al_2O_3 has a higher mechanical property after thermal shock and a higher resistance to initiate penetrating cracks than the fine-grained Al_2O_3.

The long crack depth of the two kinds of alumina versus the quench temperature experienced a rapid decrease, a slow growth, and a steady state (Fig. 6). The long
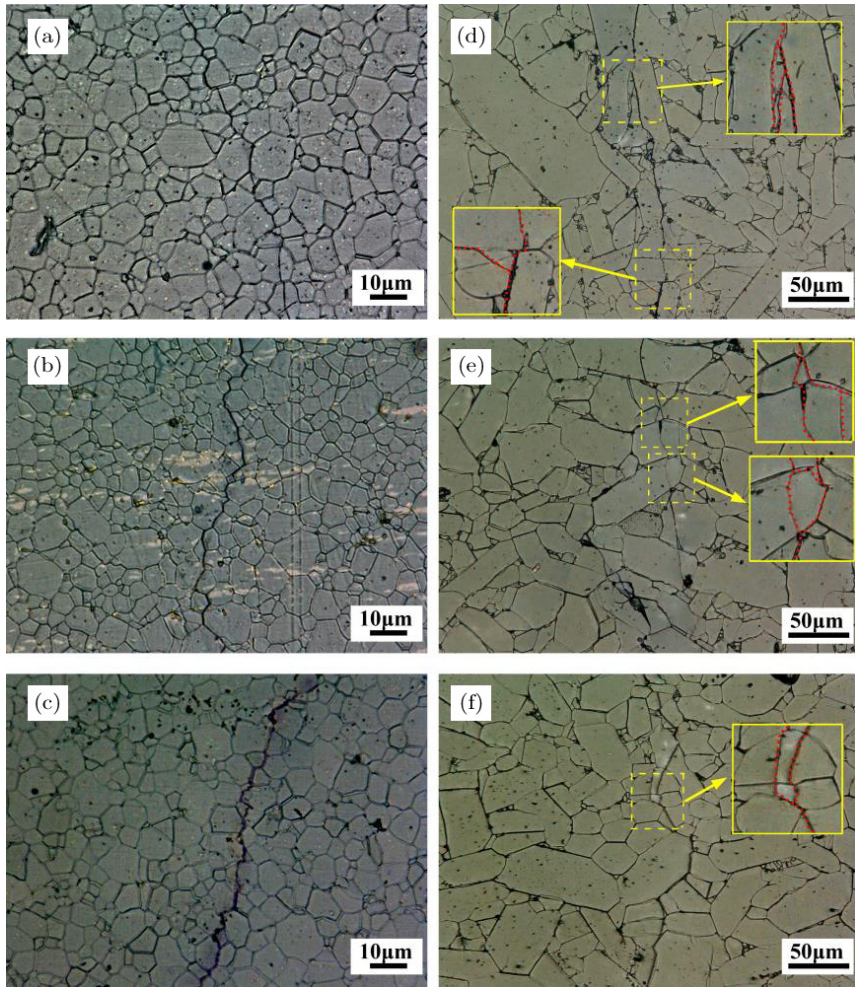
Fig. 9. Microscopic growth path of thermal-shock cracks. The arrows indicate the micro-bifurcations of the cracks. The grain size and quench temperature are (a) $4.1\,\mu m$, $300°C$; (b) $4.1\,\mu m$, $500°C$; (c) $4.1\,\mu m$, $700°C$; (d) $25.3\,\mu m$, $300°C$; (e) $25.3\,\mu m$, $500°C$ and (f) $25.3\,\mu m$, $700°C$. The dotted rectangles indicate the regions of micro-bifurcations. The area of the dotted rectangle is quadrupled to the solid rectangles. The dashed lines in the solid rectangles indicate the micro-bifurcations.

crack density of the two kinds of alumina experienced a rapid growth and a steady state as $T < 600°C$ (Fig. 7). These two features are similar to our previous study [Xu *et al.*, 2014]. However, at each quench temperature, the crack depth of the fine-grained alumina is always larger than that of the coarse-grained alumina; the crack densities of the two kinds of alumina almost have the same value as $T < 600°C$ while the density of the fine-grained alumina has a larger value than that of the coarse-grained alumina at higher quench temperature. As $600°C \leq T \leq 700°C$,

the crack density of the fine-grained alumina increased gradually while that of the coarse-grained alumina remained at the same level.

Crack initiation, propagation and bifurcation are three kinds of energy dissipation ways in the process of thermal shock (Figs. 4–7). At low quench temperature, i.e., $T < 500°C$, crack initiation or propagation are the primary forms of the energy dissipation for the two kinds of alumina. As $500°C \leq T \leq 600°C$, some long cracks of the fine-grained alumina continue to propagate and the penetrating cracks appeared, while bifurcations appeared in coarse-grained alumina. As $600°C < T \leq 700°C$, the crack density increased again and a few bifurcations appeared in fine-grained alumina, while the penetrating cracks appeared and the number of bifurcations increased in coarse-grained alumina. This indicates that the coarse-grained alumina has a better resistance to crack initiation at high quench temperature and crack propagation.

Transgranular and intergranular fracture are two kinds of microscopic fracture models of cracks propagation in polycrystalline alumina under thermal shock (Fig. 9). The microscopic fracture model is directly related to the macroscopic fracture toughness of materials. When the crack propagates along the y direction, the critical energy release rate G_{IC} and the fracture toughness K_{IC} can be expressed as [Li and Zhou, 2013],

$$G_{IC} = \frac{\partial U_f}{\partial A} = \frac{(\gamma_g l_g + \gamma_b l_b)t}{wt} = \zeta[\gamma_g \eta_g + \gamma_b(1 - \eta_g)], \tag{1}$$

$$K_{IC} = \sqrt{G_{IC}\frac{E}{1 - \nu^2}} = \sqrt{\frac{E}{1 - \nu^2}}\zeta[(\gamma_g - \gamma_b)\eta_g + \gamma_b], \tag{2}$$

where U_f is the total released energy, E is Young's modulus, ν is Poisson's ratio; γ_b and γ_g are the fracture energies per area of intergranular and transgranular fracture, respectively; $A = wt$ and w are the y-axis direction projection of the total curved crack area and length, respectively, t is the thickness of specimen; $l = l_g + l_b$ is the total curved crack length, where l_g and l_b represent the total length of the transgranular and intergranular crack, respectively (Fig. 10); $\eta_g = l_g/l$ is the transgranular proportion; the crack crooked factor $\zeta = l/w$, which is relative to the grain size and quench temperature, is employed to characterize the curving extent of crack propagation path. Under normal circumstances, the intergranular fracture energy γ_b should be less than the transgranular fracture γ_g since atomic bonding at grain boundaries maybe imperfect, impurities or grain anisotropy can result in concentrations of strain energy at the boundaries, and porosity if present is often situated at grain boundaries, and etc. [Davidge, 1974]. Obviously, it can be seen that K_{IC} is positive correlated with η_g and ζ as $\gamma_g - \gamma_b > 0$. Moreover, if γ_b, γ_g, E and ν of alumina are assumed to be independent of the grain size, K_{IC} is simply determined by the values of η_g and ζ.

Figures 11 and 12 respectively show η_g and ζ versus quench temperature for two kinds of alumina with different grain sizes. The crack path is retraced from the original microscopic image obtained by the optical microscope. After that the total
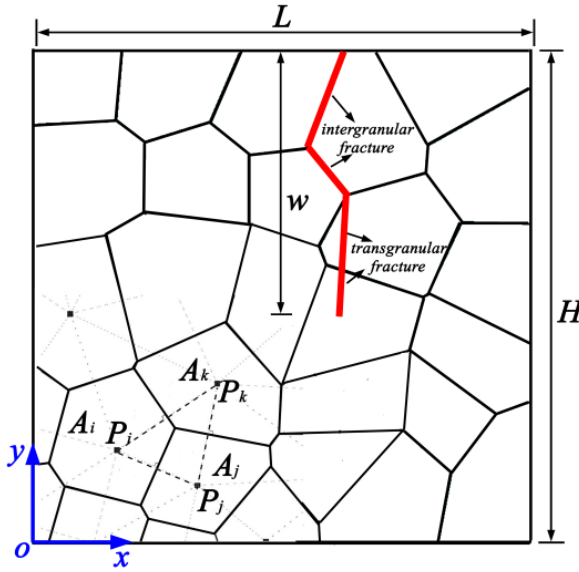
Fig. 10. Schematic of microstructure model of polycrystalline ceramic and microscopic crack propagation path. The solid and heavy solid lines represent the grain boundary and crack growth path, respectively. w is the projection length of total curved crack length in the direction of y-axis. P_i, P_j and P_k are the randomly generated discrete points on the plane, A_i, A_j and A_k are polygons composed of perpendicular bisectors of lines between two discrete points.
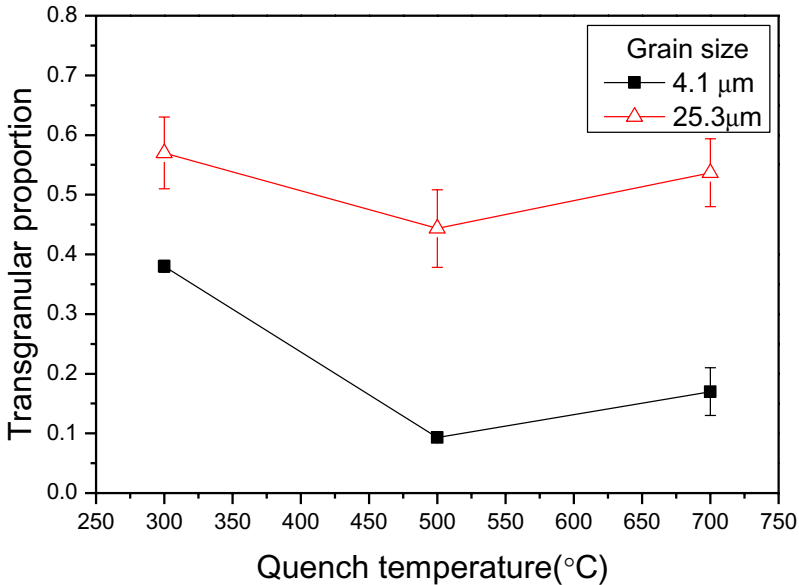

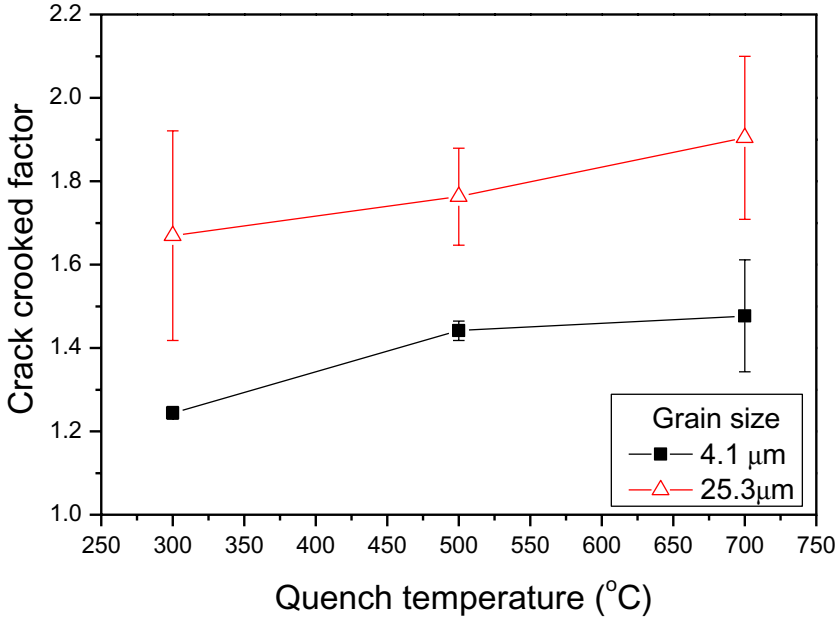Fig. 11. Transgranular fracture ratio versus quench temperature.

Fig. 12.   Crack crooked factor versus quench temperature.

length of the transgranular and intergranular crack path, l_g and l_b, are measured, respectively, the transgranular proportion η_g and crack crooked factor ζ can be obtained. Each statistical data was obtained from five cracks by random selection from the quenched samples. It can be seen that both the transgranular proportion η_g and crack crooked factor ζ of the coase-grained alumina are higher than that of the fine-grained alumina at the same quench temperature. In the case of the materials with the same grain sizes, the greater the transgranular proportion, the smaller the crack crooked factor. This is mainly because the transgranular fracture is along a straight line through a grain while the intergranular fracture is along a curve which coincided with the grain boundary. However, in the case of materials with different grain sizes, the value of ζ is determined by both η_g and micro-bifurcation. Many micro-bifurcations, indicated by arrows in Fig. 9, appeared in the coarse-grained alumina under thermal shock while few were found in fine-grained alumina. The micro-bifurcation increased the value of ζ since it can increase the total crack path and also cause a deviation from the original crack propagation path. The micro-bifurcation is the main reason the coarse-grained alumina has a higher ζ than the fine-grained alumina though it has a higher η_g. Based on Eq. (2), the coarse-grained alumina has a higher K_{IC} and exhibit a better thermal shock resistance than fine-grained alumina. This is the microscopic mechanism of the effect of grain size on thermal shock resistance of alumina.

3. Numerical Simulations

Based on the statistical mesoscopic damage mechanics [Bai *et al.*, 2006; Tang *et al.*, 2016], the crack propagation process of polycrystalline ceramic sheet subjected to thermal shock can be well simulated in our previous work [Xu *et al.*, submitted to *J. Appl. Mech.*]. A two-dimensional (2D) numerical model is introduced to depict the micro-crack propagation mechanism of ceramic sheet under water quenching (Fig. 10). The specimen dimensions along x- and y-axis are $L \times H$, where $L = 0.2$ mm and $H = 0.2$ mm. The initial temperature of the specimen is 300°C. The top surface $(y = H)$ of the sheet is quenched in water at 17°C and can be expressed by the convection boundary condition, the left surface $(x = 0)$ satisfies periodic boundary condition, the right $(x = L)$ and bottom surfaces $(y = 0)$ satisfy symmetric boundary conditions. The ceramic specimen is divided to $N = 200 \times 200$ mesoscopic units with dimensions of $1\,\mu$m $\times\ 1\,\mu$m.

The mechanical properties of the polycrystalline ceramic on the grain boundary and inner grain are different. The mesoscopic units within the specimen are divided into two groups, namely, on the grain boundary and the inner grain. For simplicity, assume the units on the grain boundary or the inner grain have the same initial strength and elastic modulus, respectively, and the ratio of their initial strength equals the ratio of their elastic modulus. Each unit is assigned to the same values of Poisson's ratio, thermal expansion coefficient, thermal conductivity, and etc. The above parameters are assumed as not changed with the temperature (Table 1) [Zhang and Ma, 2006].

Moreover, Voronoi grid method is used to construct microstructure model of polycrystalline ceramic [Zavattieri and Espinosa, 2001; Espinosa and Zavattieri, 2003]. In detail, randomly generate some discrete points $P_i, P_j, P_k, \ldots$, in the specimen, draw a line perpendicular bisector of two adjacent points, and then the plane area is divided into a number of irregular polygon shapes, such as A_i, A_j and $A_k, \ldots$ (Fig. 10). These polygons can well characterize the microstructure of the polycrystalline ceramics. Different grain sizes and shapes can be obtained by changing the number and distance of the random points (Fig. 13).

Figures 13 and 14 show the numerical simulations of micro-cracks of quenched ceramic sheet with different grain size and ratio of the initial strength of mesoscopic unit on the grain boundary to that on the inner grain. With the initial strength

Table 1. Thermal and mechanical parameters of the 99% Al$_2$O$_3$ ceramic [Zhang and Ma, 2006; Zhou *et al.*, 2012].

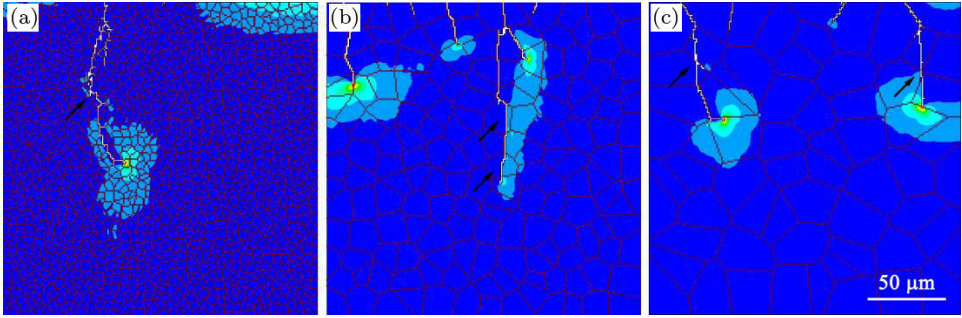| Thermal conductivity k W/(m·K)	Constant-pressure specific heat c J/(kg·K)	Coefficient of thermal expansion α K^{-1}	Density ρ kg/m^3
31	880	6.8×10^{-6}	3980
Frictional angle ϕ degree	Poisson's ratio ν	Elastic modulus E_0 GPa	Tensile strength σ_{Tc0} MPa	Biot number Bi
30	0.22	370	300	1.5

Fig. 13. Micro-crack of quenched ceramic sheet with different grain size. The mean grain sizes are: (a) $5\,\mu$m; (b) $15\,\mu$m and (c) $25\,\mu$m. The ratio initial strength of the mesoscopic unit on the grain boundary to that on the inner grain is 0.7. The black arrows indicate the transgranular propagation.
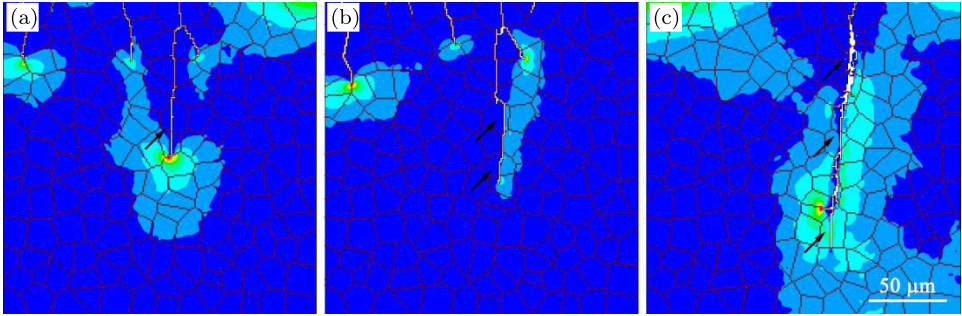

Fig. 14. Micro-crack of quenched ceramic sheet with different initial strength ratio of the mesoscopic unit on the grain boundary to that on the inner grain. The ratios are: (a) 0.6; (b) 0.7 and (c) 0.8. The mean grain size is $15\,\mu$m. The black arrows indicate the transgranular propagation.

ratio R remaining invariant, the larger the grain size is, the more likely transgranular crack happens and the transgranular proportion increases with the increase of grain size (Fig. 13). Obviously, fine-grained ceramic material is more likely to happen in intergranular fracture because that it has more number of grain boundary but shorter length of each grain boundary in the same area compared with coarse-grained ceramic. With the grain size keeping constant, transgranular proportion increases significantly as the strength ration R increases (Fig. 14). Intergranular fracture is the main fracture mode in the case of weak grain boundary. As the value of R increases, both intergranular and transagular fractures occur due to the increase of relative strength of the grain boundary. According to Eqs. (1) and (2), as the transagular proportion increases, the fracture toughness will increase and lead to higher thermal shock resistance. Therefore, the fracture toughness and thermal shock resistance can be effectively improved by strengthening grain boundary or increasing the grain size of ceramic materials.

4. Conclusion

In conclusion, a series of experiments were conducted to study the effect of grain size on thermal shock property of alumina ceramic, and a numerical model is introduced to depict the micro-crack propagation mechanism of ceramic sheet under water quenching. Thermal-shock crack and residual strength of ceramic with different grain sizes under different quench temperature have been investigated. Experimental and numerical results reveal that the grain size plays an essential role in influencing the critical thermal shock temperature, crack propagation and residual strength of alumina ceramic. Reducing the grain size of ceramic could effectively improve its critical thermal shock temperature which is mainly attributed to the higher initial strength. However, increasing the grain size might make the thermal shocked ceramic have a higher residual strength and a better resistance to crack expanding.

References

Bai, Y. L., Xia, M. F., Ke, F. J. and Li, H. L. [2006] *Damage Field Equation and Criterion for Damage Localization* (Springer, Netherlands), pp. 55–66.

Bayuseno, A. P., Latella, B. A. and O'Connor, B. H. [1999] "Resistance of alumina-spodumene ceramics to thermal shock," *J. Am. Ceram. Soc.* **82**(4), 819–824.

Carolan, D., Ivankovic, A. and Murphy, N. [2012] "Thermal shock resistance of polycrystalline cubic boron nitride," *J. Eur. Ceram. Soc.* **32**(10), 2581–2586.

Davidge, R. W. [1974] "Effects of microstructure on the mechanical properties of ceramics," in *Fracture Mechanics of Ceramics*, Vol. 2 (Plenum Press, New York), pp. 447–468.

Espinosa, H. D. and Zavattieri, P. D. [2003] "A grain level model for the study of failure initiation and evolution in polycrystalline brittle materials. Part I: Theory and numerical implementation," *Mech. Mater.* **35**(3), 333–364.

Gupta, T. K. [1972] "Strength degradation and crack propagation in thermally shocked Al_2O_3," *J Am. Ceram. Soc.* **55**(5), 249–253.

Hasselman, D. P. H. [1969] "Unified theory of thermal shock fracture initiation and crack propagation in brittle ceramics," *J. Am. Ceram. Soc.* **52**(11), 600–604.

Li, Y. and Zhou. M. [2013] "Prediction of fracturess toughness of ceramic composites as function of microstructure: II Analytical model," *J. Mech. Phys. Solids* **61**(2), 489–503.

Seaton, C. C. and Dutta, S. K. [1974] "Effect of grain-size on crack-propagation in thermally shocked B_4C," *J. Am. Ceram. Soc.* **57**(5), 228–229.

Sokal, R. R. and Michener, C. D. [1958] "A statistical method for evaluating systematic relationships," *Univ. Kans. Sci. Bull.* **38**, 1409–1438.

Tang, S. B., Zhang, H., Tang, C. A. and Liu, H. Y. [2016] "Numerical model for the cracking behavior of heterogeneous brittle solids subjected to thermal shock," *Int. J. Solids Struct.* **80**, 520–531.

Wang, L. *et al.* [2001] "Effect of size of the starting powders on the thermal shock resistance of alumina ceramics," *J. Mater. Sci. Lett.* **20**(4), 341–342.

Xu, X. H., Lin, Z. K., Sheng, S. L. and Yuan, W. J., "Evolution mechanisms of thermal shock cracks in ceramic sheet," to appear in *J. Appl. Mech.* doi:10.1115/1.4033175.

Xu, X. H., Tian, C., Sheng, S. L., Lin, Z. K. and Song, F. [2014] "Characterization of thermal-shock cracks in ceramic bars," *Sci. China-Phys. Mech. Astron.* **57**(12), 2205–2208.

You, X. Q., Si, T. Z., Liu, N., Ren, P. P., Xu, Y. and D. Feng, J. P. [2005] "Effect of grain size on thermal shock resistance of Al_2O_3–TiC ceramics," *Ceram. Int.* **31**(1), 33–38.

Zavattieri, P. D. and Espinosa, H. D. [2001] "Grain level analysis of crack initiation and propagation in brittle materials," *Acta. Mater.* **49**(20), 4291–4311.

Zhang, Y. L. and Ma, J. P. [2006] *Applicable Ceramic Material Manual[M]* (Chemical Industry Press, Beijing), pp. 337–352.

Zhou, Z. L., Song, F., Shao, Y. F., Meng, S. H., Jiang, C. P. and Li, J. [2012] "Characteristics of the surface heat transfer coefficient for Al_2O_3 ceramic in water quench," *J. Eur. Ceram. Soc.* **32**(12), 3029–3034.